

# High-resolution terahertz atmospheric water vapor continuum measurements

David M. Slocum,<sup>\*</sup> Thomas M. Goyette, and Robert H. Giles

Submillimeter-Wave Technology Laboratory, University of Massachusetts Lowell, Lowell, MA  
01854, United States

## ABSTRACT

The terahertz frequency regime is often used as the ‘chemical fingerprint’ region of the electromagnetic spectrum due to the large number of rotational and vibrational transitions of many molecules of interest. This region of the spectrum has particular utility for applications such as pollution monitoring and the detection of energetic chemicals using remote sensing over long path lengths through the atmosphere. Although there has been much attention to atmospheric effects over narrow frequency windows, accurate measurements across a wide spectrum are lacking. The water vapor continuum absorption is an excess absorption that is unaccounted for in resonant line spectrum simulations. Currently a semi-empirical model is employed to account for this absorption, however more measurements are necessary to properly describe the continuum absorption in this region. Fourier Transform Spectroscopy measurements from previous work are enhanced with high-resolution broadband measurements in the atmospheric transmission window at 1.5THz. The transmission of broadband terahertz radiation through pure water vapor as well as air with varying relative humidity levels was recorded for multiple path lengths. The pure water vapor measurements provide accurate determination of the line broadening parameters and experimental measurements of the transition strengths of the lines in the frequency region. Also these measurements coupled with the atmospheric air measurements allow the water vapor continuum absorption to be independently identified at 1.5THz. Simulations from an atmospheric absorption model using parameters from the HITRAN database are compared with the current and previous experimental results.

Keywords: water vapor; continuum; absorption; terahertz; spectroscopy

## INTRODUCTION

The main source of atmospheric opacity in the terahertz regime is water vapor. There is strong absorption at the resonant frequencies of the rotational absorption lines as well as significant absorption in the atmospheric windows between the lines caused by the far wings of the absorption peaks. However, there is a discrepancy between theoretical models and experimental observations of the amount of absorption in these windows. An empirical continuum term is added to the models to account for this discrepancy. Much work has been performed to identify the functional form of the continuum contribution<sup>1-5</sup> in the terahertz region, where the most frequently used expression has a quadratic dependence on frequency and a negative temperature dependence. There is much more ambiguity in the continuum parameters themselves as the continuum parameters obtained in any study are heavily dependent on a number of factors including the line shape function, line parameters, and number of lines used in the model.

The water vapor spectrum has been extensively studied, but until recently the terahertz region has received little attention for experimental studies and broadband investigations are lacking. A few broadband studies have been performed using atmospheric air,<sup>6-9</sup> however these studies lack control over the experimental parameters and fail to cover the whole parameter space. Other authors have performed broadband studies in laboratory conditions using either pure nitrogen or oxygen as a broadening agent,<sup>10-14</sup> however more investigations are necessary for a full analysis of the water vapor continuum.

---

<sup>\*</sup> Corresponding author. Email: David\_Slocum@student.uml.edu phone: 978-934-1300 www.stl.uml.edu

The current study expands on previous work<sup>15,16</sup> of a broadband Fourier Transform Spectroscopy study using dry air as a broadening agent. High-resolution data were taken in the atmospheric transmission window at 1.5THz over multiple path lengths and pressures. The resulting transmission spectra were fitted to a Van Vleck-Weisskopf line shape using the line parameters from the 2008 HITRAN Database<sup>17</sup> (HITRAN) with an added empirical continuum term.

### PROCEDURE

Transmission data were collected using a variable path-length White cell. A detailed description of the cell can be found in Ref. [15]. A 1.5THz frequency multiplied source and sub-harmonic mixing receiver from Virginia Diodes Inc. were utilized to produce and collect the terahertz radiation. The source and receiver were coherent instruments, allowing for the collection of both the magnitude and phase of the electric field using a dual channel digital RF Lock In Amplifier with a time constant of 100μs after passing through a down converting RF chain. A schematic of the experimental setup is shown in Figure 1.

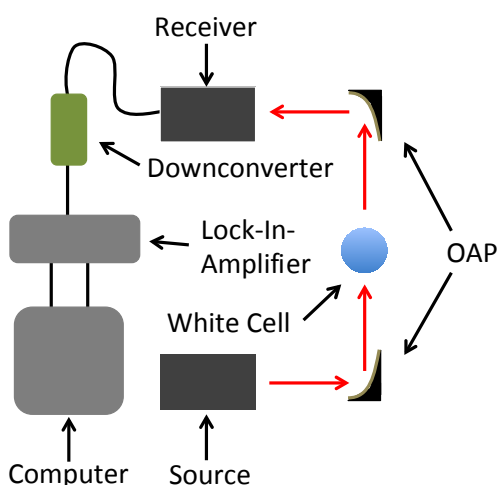


Figure 1. Schematic of the experiment setup.

The experimental setup was located in a temperature and humidity controlled laboratory with the ambient temperature at 297K. For a single data set the path length of the cell was held constant and the cell was evacuated to below 20mTorr and sealed. Two background scans were completed with the sealed evacuated cell. The scans included a closed background with the source blocked and an open background with the source radiation propagating through the setup. Distilled water vapor was then released into the cell to the desired pressure. After the system had come to equilibrium a sample scan was completed and more distilled water vapor was released into the cell. The process of releasing water vapor and taking scans was repeated five times for each path length at approximately 2, 5, 9, 12, and 15Torr. A total of six path lengths were investigated: 1, 2, 3, 5, 6, and 8m. The exact conditions for each data set are listed in Table 1.

Table 1. A list of the water vapor pressures in Torr and corresponding propagation lengths for each data set in the study.

1m	2m	3m	5m	6m	8m
1.54	2.32	1.94	2.23	1.98	2.57
4.48	4.98	4.90	4.91	4.81	4.85
8.52	8.87	8.85	8.92	9.04	8.40
11.1	14.4	12.0	11.5	11.5	11.4
14.6	15.4	14.6	14.4	14.5	15.2

## RESULTS

The raw data collected from the experiment exhibited a number of interfering signals from ambient sources and reflections superimposed on it. A number of data processing routines were applied to the data to extract the absorption measurements from the noise. The complex closed background was first subtracted to remove any signals not being produced directly by the source. Next the mean value of the complex data set was subtracted to remove any signal with stationary phase. After that the data was Fourier Transformed into distance space and a notch filter was applied to remove any spurious signals near the main peak. Finally a range gate was applied to the data to isolate data that had traveled the appropriate distance through the setup. The range gating process is depicted in Figure 2 for a simulated data set. The range gating process is depicted in Figure 2 for a simulated data set. The Fourier Transform of the signal is shown in Figure 2a with the main peak at 1.72m. In Figure 2b a Gaussian window centered on the main peak was applied to the Fourier Transform of the signal to accomplish the range gating. After the window is applied the data is then transformed back to frequency space.

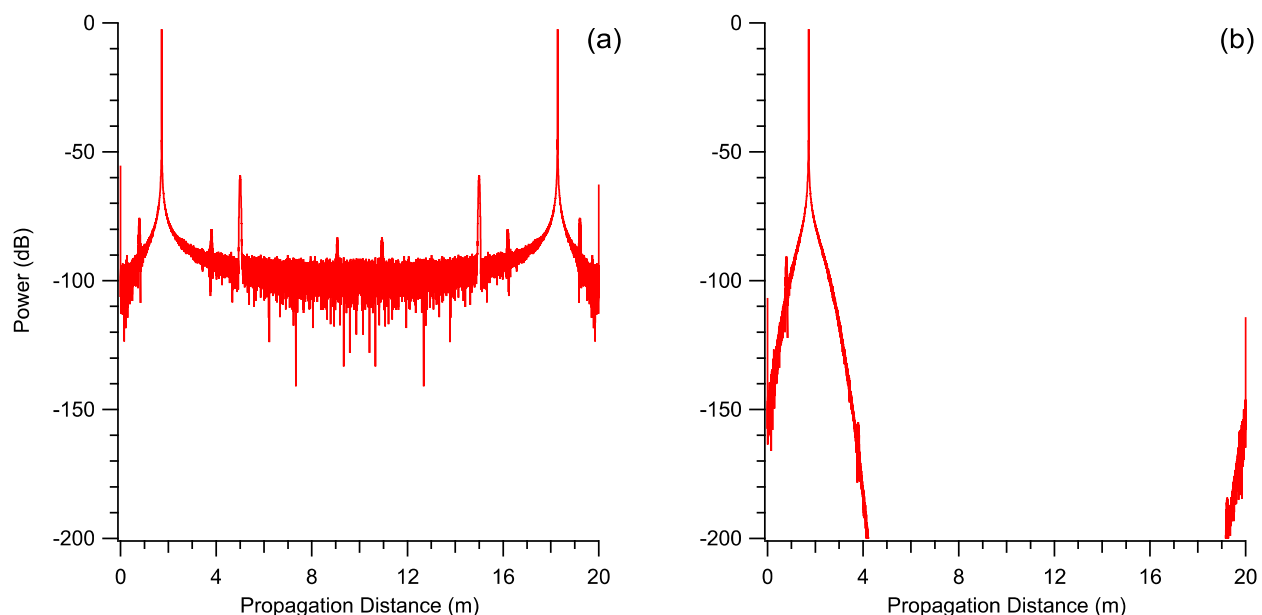


Figure 2. (a) An FFT of a simulated data set with a main peak at 1.72m and (b) an applied range gate to the FFT.

Figure 3 shows a plot of the experimental transmission spectrum of 4.85Torr of water vapor and a propagation length of 8m. The red plot shows the raw transmission data while the black plot shows the transmission after passing through all of the processing mathematics. As shown in the figure, the presence of the two absorption peaks cannot be discerned in the raw data but are clearly identifiable in the processed data.

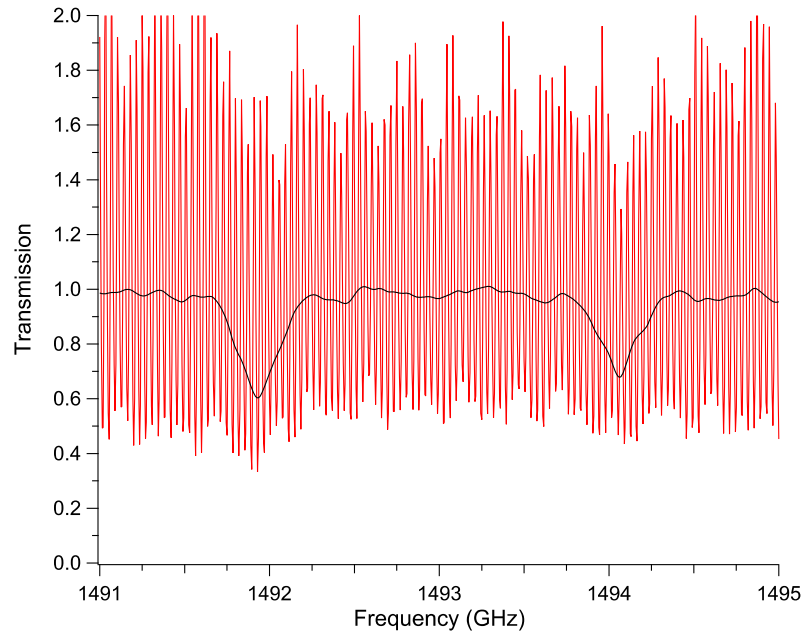


Figure 3. A plot of the pre- (red) and post-processed (black) transmission for a propagation length of 8m and a pressure of 4.85Torr. The periodic scintillation is due to interfering signals beating with the desired signal.

The processing routine outlined above was applied identically to both the sample scans and the corresponding open background scans. The transmission was then calculated by normalizing the sample scans to the open background scans. Finally the transmission data was corrected to remove any distortions acquired from the range gating mathematics. Figure 4a shows a simulated self broadened transmission spectrum of 2Torr of water vapor with a propagation length of 8m. The black plot is the original simulated spectrum while the red plot is the same spectrum after passing through the range gating mathematics. It can be seen that the line shape is significantly distorted and a correction is necessary to recover the true line shape. Figure 4b shows an experimental self broadened transmission spectrum of 2.57Torr of water vapor with a propagation length of 8m. The red plot is the experimental transmission after passing through the processing routines described above while the black plot is that processed transmission after accounting for the range gate distortion. As can be seen in Figure 4, the range gating mathematics distorts the absorption peaks lowering the peak amplitude and broadening the width while having little effect on the continuum between the lines. The distortion applied by the range gating mathematics can be removed by use of the convolution theorem of Fourier Transforms, Eq. ( 1 )

$$h(x) = l(x)d(x) = (f * g)(x) = \int f(y)g(x - y)dy \quad (1)$$

$$\mathcal{F}\{h(x)\} = \mathcal{F}\{f(x)\}\mathcal{F}\{g(x)\}$$

The ideal line shape function, Eq. ( 2 ), can be found as

$$l(x) = \frac{\mathcal{F}^{-1}\{\mathcal{F}\{f(x)\}\mathcal{F}\{g(x)\}\}}{d(x)} \quad (2)$$

In Eqs. ( 1 ) and ( 2 )  $l(x)$  is the ideal line shape function,  $d(x)$  is a distortion function,  $f(x)$  is the input spectrum, and  $\mathcal{F}\{g(x)\}$  is the applied window. The distortion function can be found by use of a test function and solving for  $d(x)$  instead of  $l(x)$  in Eq. ( 2 ).

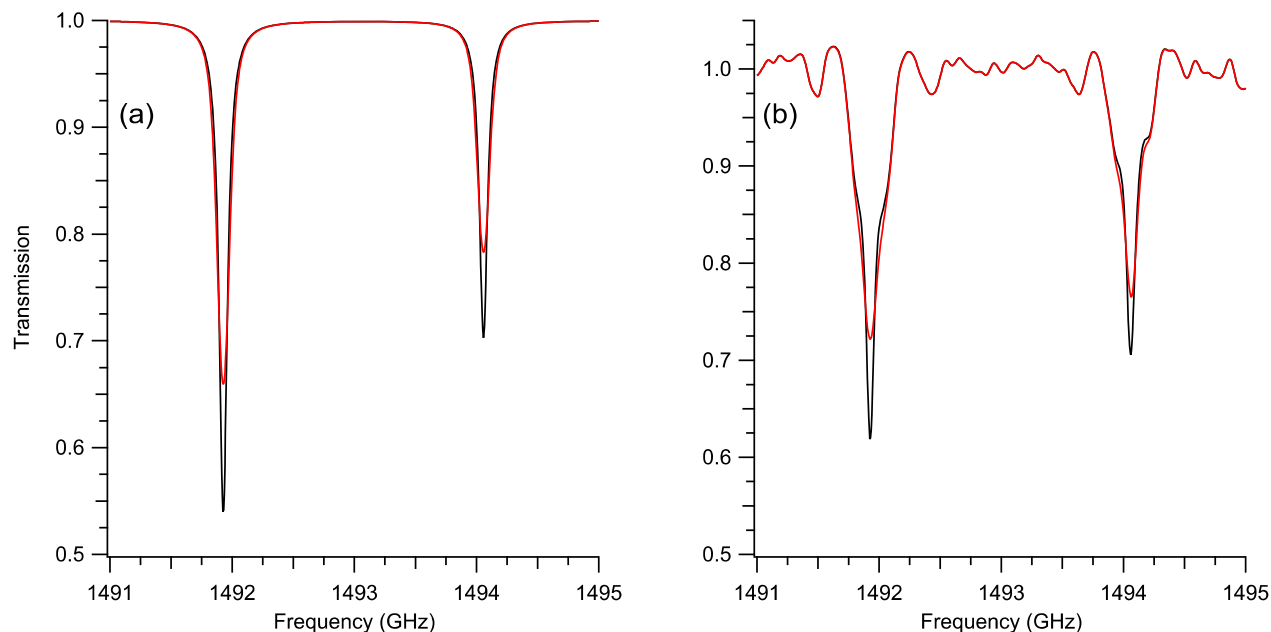


Figure 4. (a) Simulated transmission for a propagating length of 8m and a pressure of 2Torr of water vapor. The simulated transmission before (black) and after (red) applying the range gating routine. (b) Experimental transmission for a propagation length of 8m and a pressure of 2.57Torr. The transmission before (red) and after (black) correcting for the range gate distortion.

## DISCUSSION

Once the transmission of the sample was found, it was fitted to the Beer-Lambert Law given by

$$\tau(\nu) = \exp \{-l(\alpha_l(\nu) + \alpha_c(\nu))\} \quad (3)$$

In Eq. ( 3 ),  $\tau$  is the normalized transmission,  $\nu$  is the frequency in MHz,  $\alpha_l$  is the resonant line absorption coefficient in  $\text{m}^{-1}$ , and  $\alpha_c$  is the continuum contribution to the absorption coefficient in  $\text{m}^{-1}$ . The resonant absorption line spectrum is a sum over each absorption line in the region, which is given by a Van Vleck-Weisskopf line shape<sup>18</sup>

$$\alpha_k(\nu) = \alpha_{k,max} \frac{\nu}{\nu_k} \left( \frac{1}{\left(\frac{\nu-\nu_k}{\Delta\nu_k}\right)^2 + 1} + \frac{1}{\left(\frac{\nu+\nu_k}{\Delta\nu_k}\right)^2 + 1} \right) \quad (4)$$

The continuum contribution to the absorption coefficient<sup>18</sup> is given by Eq. ( 5 )

$$\alpha_c(\nu) = \nu^2 P_s (P_s C_s \theta^{n_s} + P_f C_f \theta^{n_f}) \quad (5)$$

In Eqs. ( 4 ) and ( 5 ),  $\alpha_k$  is the absorption coefficient due to one resonant absorption line in  $\text{m}^{-1}$ ,  $\alpha_{k,max}$  is the peak amplitude of the self broadened absorption line in  $\text{m}^{-1}$ ,  $\nu_k$  is the resonance frequency of the absorption line in MHz,  $\Delta\nu_k$  is the half width at half max of the absorption line in MHz,  $P_s$  and  $P_f$  are the pressures of the water vapor and foreign gas in Torr, and  $C_s$  and  $C_f$  are the self and foreign continuum coefficients in  $\text{m}^{-1}/(\text{Torr}^2\text{MHz}^2)$ . The line strength,  $I_k$  in  $\text{nm}^2\text{MHz}$ , and the self and foreign gas line broadening coefficients,  $\gamma_{ks}$ , and  $\gamma_{kf}$  in MHz/Torr, are related to the fitting parameters  $\alpha_{k,max}$  and  $\Delta\nu_k$  by the relations

$$\begin{aligned} \alpha_{k,max} &= 10,245.8(I_k/\gamma_{ks}) \\ \Delta\nu_k &= \gamma_{ks}P_s + \gamma_{kf}P_f \end{aligned} \quad (6)$$

Using Eqs.( 3 )-( 6 ), the line strength and self broadening parameter were determined for several strong absorption lines in the region of interest. The experimental values were found by a least squares fit of Eq. ( 3 ) to all of the experimental transmission spectra in the study. The line parameters resulting from the fitting are displayed in Table 2 along with the corresponding HITRAN values. Figure 5 shows a plot of the fit for two absorption lines in the frequency region of interest. The transmission data is for a propagation length of 8m and pressures of 2.57, 4.85, 8.40, 11.4, and 15.2Torr.

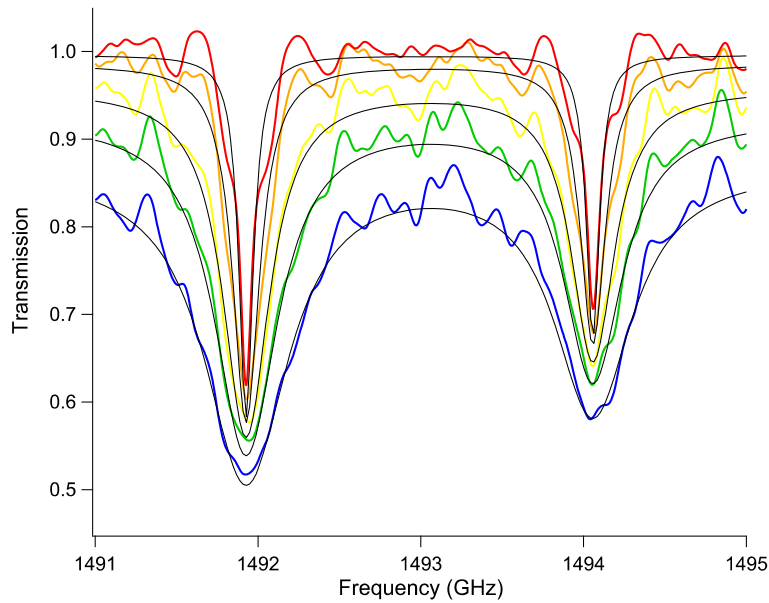


Figure 5. Plot of the experimental transmission data for a propagation length of 8m and pressures of 2.57, 4.85, 8.40, 11.4, and 15.2Torr for the red, orange, yellow, green, and blue plots respectively. The fits to these plots are all shown in black.

The self continuum coefficient was also determined from the fitting of Eqs. ( 3 )-( 6 ) to the experimental transmission. The self continuum coefficient was determined to be  $1.498(3) \times 10^{-17} \text{ m}^{-1}/(\text{Torr}^2\text{MHz}^2)$  from a fit to the 2, 3, 5, 6, and 8m data sets, where the reported error is the statistical error from the fitting routine. Figure 6 shows a plot of the fit for the continuum in the frequency region of interest. The transmission data is shown with a propagation length of 5m and pressures of 2.23, 4.91, 8.92, 11.5, and 14.4Torr. The current value for  $C_s$  is in relatively good agreement with the value obtained by Podobedov et al.<sup>11,12</sup> of  $C_s=1.57 \times 10^{-17} \text{ m}^{-1}/(\text{Torr}^2\text{MHz}^2)$ . The frequency regions of interest for this study and the work of Podobedov et al. overlapped, and the other experimental conditions similarly had sufficient overlap for a direct comparison. Other authors<sup>13,14,18</sup> have obtained values of  $C_s$  significantly larger ranging from  $3.258\text{-}3.9 \times 10^{-17} \text{ m}^{-1}/(\text{Torr}^2\text{MHz}^2)$ , however the experimental conditions of these studies did not correspond to the current study parameters.

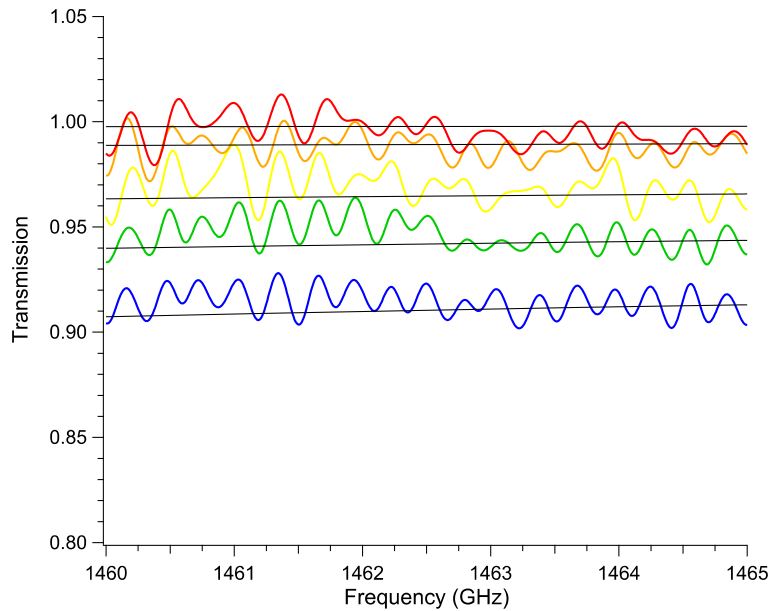


Figure 6. Plot of the experimental transmission data for a propagation length of 5m and pressures of 2.23, 4.91, 8.92, 11.5, and 14.4Torr for the red, orange, yellow, green, and blue plots respectively. The fits to all of the plots are shown in black.

The current value for  $C_s$  was used to reanalyze previous broadband air broadened water vapor absorption measurements.<sup>15</sup> Using the same fitting routine as described in Ref [15] a value of  $C_f=1.18 \times 10^{-18} \text{m}^{-1}/(\text{Torr}^2 \text{MHz}^2)$  was obtained, which is in agreement with the previously determined value of  $C_f=1.16 \times 10^{-18} \text{m}^{-1}/(\text{Torr}^2 \text{MHz}^2)$  to within uncertainty. The new continuum parameter set resulted in the same spectra as previously determined as the change in the continuum contribution from the new parameter set was 0.30%.

Table 2. Experimentally determined line parameters using 30 data sets. The frequency is given in MHz, the line strengths are given in  $\text{nm}^2 \text{MHz}$ , and the line broadening coefficients are given in  $\text{MHz/Torr}$ . The reported error is the statistical error from the fitting routine.

HITRAN Frequency	$I_k$	HITRAN $I_k$	Percent Difference	$\gamma_{ks}$	HITRAN $\gamma_{ks}$	Percent Difference
1491927	$1.18(1) \times 10^{-4}$	$1.27 \times 10^{-4}$	6.5	18.1(3)	17.5	3.4
1494257	$8.37(11) \times 10^{-5}$	$8.27 \times 10^{-5}$	1.2	17.5(3)	18.0	2.8
1541967	$5.07(5) \times 10^{-3}$	$4.59 \times 10^{-3}$	10	16.3(2)	17.6	7.4

## CONCLUSIONS

Presented in this paper are high-resolution broadband absorption measurements of water vapor of varying pressures and propagation lengths. Absorption data were recorded using a frequency-multiplied source, sub-harmonic mixing receiver, and variable path length White cell. The raw data were passed through multiple mathematical processing routines to extract the transmission spectra from interfering signals. These processed transmission spectra were fitted to absorption spectra using a Van Vleck-Weisskopf line shape. From the fitting routine the line strength and self broadening parameter for several absorption lines were determined, which were compared with values from HITRAN. The fitting routine also allowed for the determination of the self broadened continuum coefficient. The value obtained for  $C_s$  was  $1.498 \times 10^{-17} \text{m}^{-1}/(\text{Torr}^2 \text{MHz}^2)$ , which is in relatively good agreement with the value obtained by other authors<sup>11,12</sup> investigating the frequency region of interest.

## REFERENCES

- [ 1 ] Ma, Q. and Tipping, R. H., "Water vapor continuum in the millimeter spectral region," *J. Chem. Phys.* 93(9), 6127-6139 (1990).
- [ 2 ] Liebe, H. J., "MPM-An Atmospheric Millimeter-Wave Propagation Model," *Int. J. Infrared Milli Waves* 10(6), 631-650 (1989).
- [ 3 ] Liebe, H. J., Hufford, G. A. and Cotton, M. G., "Propagation Modeling Of Moist Air and Suspended Water/Ice Particles at Frequencies Below 1000 GHz," *Proceedings of the AGARD 52nd Specialists Meeting of the Electromagnetic Wave Propagation Panel, Palma de Mallorca, Spain* (1993).
- [ 4 ] Pardo, J. R., Cernicharo, J. and Serabyn, E., "Atmospheric Transmission at Microwaves (ATM): An Improved Model for Millimeter/Submillimeter Applications," *IEEE T Antenn. Propag.* 49(12), 1683-1694 (2001).
- [ 5 ] Rosenkranz, P. W., "Water vapor microwave continuum absorption: A comparison of measurements and models," *Rad. Sci.* 33(4), 919-928 (1998).
- [ 6 ] Pardo, J. R., Serabyn, E. and Cernicharo, J., "Submillimeter atmospheric transmission measurements on Mauna Kea during extremely dry El Nino conditions: implications for broadband opacity contributions," *JQSRT* 68(4), 419-433 (2001).
- [ 7 ] Serabyn, E., Weisstein, E. W., Lis, D. C. and Pardo, J. R., "Submillimeter Fourier-transform spectrometer measurements of atmospheric opacity above Mauna Kea," *Appl. Opt.* 37(12), 2185-2198 (1998).
- [ 8 ] Matsuo, H., Sakamoto, A. and Matsushita, S., "FTS Measurements of Submillimeter-Wave Atmospheric Opacity at Pampa la Bola," *Publ. Astron. Soc. Japan* 50, 359-366 (1998).
- [ 9 ] Paine, S., Blundell, R., Papa, D. C., Barrett, J. W. and Radford, S. J. E., "A Fourier Transform Spectrometer for Measurement of Atmospheric Transmission at Submillimeter Wavelengths," *Publ. Astron. Soc. Pacific* 112, 108-118 (2000).
- [ 10 ] Burch, D. E., "Absorption of Infrared Radiant Energy by CO<sub>2</sub> and H<sub>2</sub>O. III. Absorption by H<sub>2</sub>O between 0.5 and 36 cm<sup>-1</sup> (278 μ-2 cm)," *J. Opt. Soc. Am.* 58(10), 1383-1394 (1968).
- [ 11 ] Podobedov, V. B., Plusquellic, D. F., Siegrist, K. E., Fraser, G. T., Ma, Q., and Tipping, R. H., "New Measurements of the water vapor continuum in the region from 0.3 to 2.7THz," *JQSRT* 109(3), 458-467 (2008).
- [ 12 ] Podobedov, V. B., Plusquellic, D. F., Siegrist, K. M., Fraser, G. T., Ma, Q. and Tipping, R. H., "Continuum and magnetic dipole absorption of the water vapor-oxygen mixtures from 0.3 to 3.6 THz," *J. Mol. Spec.* 251(1-2), 203-209 (2008).
- [ 13 ] Koshelev, M. A., Serov, E. A., Parshin, V. V., and Tretyakov, M. Y., "Millimeter wave continuum absorption in moist nitrogen at temperatures 261-328K," *JQSRT* 112(17), 2704-2712 (2011).
- [ 14 ] Yang, Y., Mandehgar, M., and Grischkowsky, D., "Determination of the water vapor continuum absorption by THz-TDS and molecular response theory," *Opt. Express* 22(4), 4388-4403 (2014).
- [ 15 ] Slocum, D. M., Slingerland, E. J., Giles, R. H., and Goyette, T. M., "Atmospheric absorption of terahertz radiation and water vapor continuum effects," *JQSRT* 127, 49-63 (2013).
- [ 16 ] Slocum, D. M., Goyette, T. M., Slingerland, E. J., Giles, R. H., and Nixon, W. E., "Terahertz atmospheric attenuation and continuum effects," *Proc. SPIE 8716, Terahertz Physics, Devices, and Systems VII: Advanced Applications in Industry and Defense*, 871607 (2013).

- [ 17 ] Rothman, L. S., Gordon, I. E., Barbe, A., Chris Benner, D., Bernath, P. F., Birk, M., Boudon, V., Brown, L. R., Campargue, A., Champion, J. P., Chance, K., Coudert, L. H., Dana, V., Devi, V. M., Fally, S., Flaud, J. M., Gamache, R. R., Goldman, A., Jacquemart, D., Kleiner, I., Lacombe, N., Lafferty, W. J., Mandin, J. Y., Massie, S. T., Mikhailenko, S. N., Miller, C. E., Moazzen-Ahmadi, N., Naumenko, O. V., Nikitin, A. V., Orphal, J., Perevalov, V. I., Perrin, A., Predoi-Cross, A., Rinsland, C. P., Rotger, M., Simeckova, M., Smith, M. A. H., Sung, K., Tashkun, S. A., Tennyson, J., Toth, R. A., Vandaele, A. C. and Vander Auwera, J., "The HITRAN 2008 molecular spectroscopic database," *JQSRT* 110(9-10), 533-572 (2009).
- [ 18 ] Kuhn, T., Bauer, A., Godon, M., Buhler, S. and Kunzi, K., "Water vapor continuum: absorption measurements at 350GHz and model calculations," *JQSRT* 74(5), 545-562 (2002).